Hindawi Publishing Corporation
EURASIP Journal on Advances in Signal Processing
Volume 2007, Article ID 45364, 11 pages
doi:10.1155/2007/45364

Research Article

Carrier Frequency Offset Estimation and I/Q Imbalance Compensation for OFDM Systems

Feng Yan, Wei-Ping Zhu, and M. Omair Ahmad

Centre for Signal Processing and Communications, Department of Electrical and Computer Engineering, Concordia University, Montreal, Quebec, Canada H3G 1M8

Received 18 October 2005; Revised 28 November 2006; Accepted 11 January 2007

Recommended by Richard J. Barton

Two types of radio-frequency front-end imperfections, that is, carrier frequency offset and the inphase/quadrature (I/Q) imbalance are considered for orthogonal frequency division multiplexing (OFDM) communication systems. A preamble-assisted carrier frequency estimator is proposed along with an I/Q imbalance compensation scheme. The new frequency estimator reveals the relationship between the inphase and the quadrature components of the received preamble and extracts the frequency offset from the phase shift caused by the frequency offset and the cross-talk interference due to the I/Q imbalance. The proposed frequency estimation algorithm is fast, efficient, and robust to I/Q imbalance. An I/Q imbalance estimation/compensation algorithm is also presented by solving a least-square problem formulated using the same preamble as employed for the frequency offset estimation. The computational complexity of the I/Q estimation scheme is further reduced by using part of the short symbols with a little sacrifice in the estimation accuracy. Computer simulation and comparison with some of the existing algorithms are conducted, showing the effectiveness of the proposed method.

1. INTRODUCTION

Orthogonal frequency division multiplexing (OFDM) technique has been extensively used in communication systems such as wireless local area networks (WLAN) and digital broadcasting systems. Three WLAN standards, namely, the IEEE802.11a, the HiperLAN/2, and the mobile multimedia access communication (MMAC), have adopted OFDM [1]. The first two standards are commonly used in North America and Europe, and the last one is recommended in Japan. In addition to WLAN, two European broadcasting systems, namely, the digital audio broadcasting (DAB) system and the digital terrestrial TV broadcasting (DVB) system, have also employed OFDM technique.

An OFDM communication system is able to cope well with frequency selective fading and thus makes an effective transmission of high-bit-rate data over wireless channels possible. However, it is very sensitive to carrier frequency offset that is usually caused by the motion of mobile terminal or the frequency instability of the oscillator in the transmitter and/or the receiver. The carrier frequency offset destroys the orthogonality among the subcarriers in OFDM systems and gives rise to interchannel interference (ICI). A practical OFDM system can only tolerate a frequency error that is approximately one percent of the subcarrier bandwidth, implying that the frequency synchronization task in OFDM systems is more critical compared with other communication systems [1–3].

To counteract the carrier frequency offset, some estimation techniques have been proposed in literature. They can be broadly classified into data-aided and non-data-aided schemes depending on whether or not a training sequence is used. Generally speaking, non-data-aided algorithms are more suitable for continuous transmission systems while data-aided techniques are often used in burst mode systems. In [2, 4, 5], non-data-aided schemes using cyclic prefix or null subcarriers have been presented. However, these algorithms need a large computational amount to cope with multipath fading. A few data-aided techniques have been proposed in [3, 6, 7], in which training sequences are used in conjunction with classical estimation theory to determine the carrier frequency offset. Although the data-aided estimators consume additional bandwidth, their estimation performances are better than non-data-aided ones, especially in multipath fading environments. For example, using training data, the maximum likelihood estimator can provide a fast

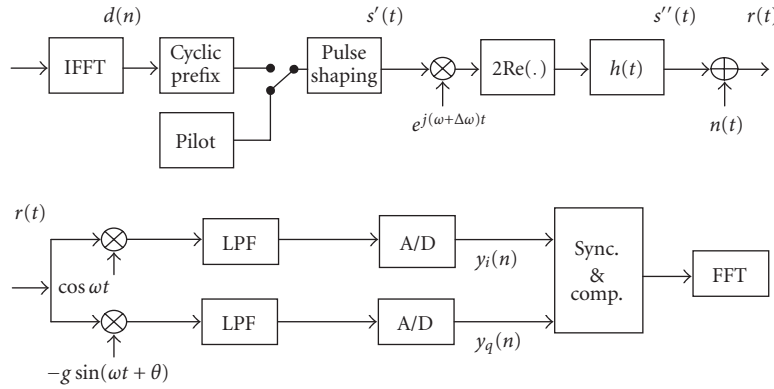

Figure 1: Block diagram of the transmitter and receiver in the OFDM system.

and efficient estimation with low implementation complexity. However, the common drawback of most of the existing algorithms is that they do not take into account the effect of inphase/quadrature (I/Q) imbalance which is a common radio frequency (RF) imperfection in real communication systems [8]. In fact, conventional frequency estimators which have not taken into account the I/Q imperfection would lead to poor estimation accuracy. Some of them can hardly work in presence of I/Q imbalance [9]. The impact of I/Q imbalance on QPSK OFDM systems was studied in [10]. An analysis of the impact of I/Q imbalance on CFO estimation in OFDM systems has also been given in [11].

The I/Q imbalance refers to both the amplitude and the phase errors between the inphase (I) and quadrature (Q) branches in analog quadrature demodulators. The amplitude imbalance arises from the gain mismatch between I and Q branches, while the phase imbalance is caused by the nonorthogonality of the I and Q branches. Any amplitude and phase imbalance would result in incomplete image rejection, especially in the direct conversion receiver which demodulates the RF signal to its baseband version directly. With state-of-the-art analog design technology, local mixer in the receiver still gives about 2% amplitude and phase imbalance [12]. This deviation would result in $20 \sim 40$ dB image attenuation only.

Recently, direct-conversion analog receiver has received a great deal of attention [12]. It is increasingly becoming a promising candidate for monolithic integration, since it avoids the costly intermediate filter in IF quadrature architecture and allows for an easy integration compared to a digital I/Q architecture which normally needs a very high sampling rate and high-performance filters.

Traditionally, the I/Q imbalance is compensated by adaptive filters [8, 12–14]. An adaptive filter can provide a very good compensation in continuous transmission systems after an initial period of tens of OFDM symbols. However, the long convergence time of adaptive filters is critical in burst-mode systems, since it is usually longer than the whole frame duration. A few I/Q imbalance estimation algorithms without using adaptive filters have been proposed in [15, 16]. But these algorithms have assumed no carrier frequency offset, and therefore, they do not work properly if the frequency offset is present. More recently, several frequency offset estimation algorithms that consider the effect of I/Q imbalance have been developed in [9, 17–19]. However, the methods proposed in [17, 18] give a quite large mean-square estimation error, while the algorithm in [9] requires intensive computations in order to achieve a good estimation result. On the other hand, the scheme suggested in [19] needs channel estimation.

The objective of this paper is to propose standard-compatible frequency estimation and I/Q imbalance compensation algorithms by using the preamble defined in IEEE 802.11a [6, 9]. A system model with the carrier frequency offset and I/Q imbalance is first addressed. A frequency estimation algorithm and an I/Q imbalance compensation scheme are then derived. The proposed estimation methods are also analyzed and computer simulated, showing the performance of the new algorithms in comparison to some of the existing techniques.

2. SYSTEM MODEL WITH CFO AND I/Q IMBALANCE

Figure 1 shows a direct-convention OFDM communication system in which both the carrier frequency offset (CFO) and the I/Q imbalance are involved. In the transmitter, an inverse fast Fourier transform (IFFT) of size N is used for modulation, and a complex-valued preamble (pilot signal) containing P short symbols, denoted by $p(t)$, is pulse shaped using an analog shaping filter $g_t(t)$. Thus, the transmitted pilot signal can be written as

$$s'(t) = p(t) \otimes g_t(t), \tag{1}$$

where $\otimes$ denotes the convolution. After passing through a frequency selective fading channel and the RF modulation with a carrier frequency offset $\Delta\omega$, the passband pilot signal $s''(t)$ can be written as

$$\begin{aligned} s''(t) &= 2\,\mathrm{Re}\left\{[s'(t) \otimes h'(t)]e^{j(\Delta\omega+\omega)t}\right\} \\ &= 2\,\mathrm{Re}\left\{[s(t)]e^{j(\Delta\omega+\omega)t}\right\}, \end{aligned} \tag{2}$$

where $\mathrm{Re}\{\cdot\}$ denotes the real part, ω the carrier frequency,

and $s(t)$ the distorted version of the transmitted signal $s'(t)$. Note that $h'(t)$ can be regarded as the baseband equivalent of the passband impulse response $h(t)$ of the channel, which satisfies $h(t) = 2\,\mathrm{Re}[h'(t)e^{j(\Delta\omega+\omega)t}]$.

In the front end of the receiver, the received signal $r(t)$ can be written as

$$\begin{aligned} r(t) &= 2\,\mathrm{Re}\left[s(t)e^{j(\omega+\Delta\omega)t}\right] + n(t) \\ &= 2s_i(t)\cos(\omega+\Delta\omega)t - 2s_q(t)\sin(\omega+\Delta\omega)t + n(t), \end{aligned} \tag{3}$$

where $s_i(t)$ and $s_q(t)$ are the inphase and the quadrature components of $s(t)$, respectively, and $n(t)$ is additive noise. In the receiver, an RF demodulator with the I/Q imbalance characterized by the amplitude mismatch g and the angular error θ is employed. The Sync & Comp (synchronizations and compensations) module is used to perform the carrier frequency synchronization as well as the I/Q compensation task. The received signal passes through an RF demodulator with the I/Q imbalance, and is then processed by the low-pass filter (LPF) and the A/D converter.

We first assume that the OFDM system suffers from the carrier frequency offset only. The output of the A/D converter, that is, the received baseband signal $\hat{y}(n)$ can be given by

$$\hat{y}(n) = s(n)e^{j\varphi n} + w(n), \tag{4}$$

where $\varphi = \Delta\omega T_s$ with T_s being the sampling period, and $w(n)$ is assumed as additive white Gaussian noise (AWGN). The received signal $\hat{y}(n)$ can be regarded as the rotated version of $s(t)$. If the channel is ideal, $s(t)$ is simply the transmitted baseband signal. Consequently, the classical estimators, such as the maximum likelihood algorithm, the least-square algorithm, can be easily applied to (4) in order to estimate the carrier frequency offset [2–7].

Next we assume that the OFDM system contains the I/Q imbalance only, that is, there is no carrier frequency offset involved. The received signal $\tilde{y}(n)$ can then be given by [12]

$$\tilde{y}(n) = K_1 s(n) + K_2 s^*(n) + w(n), \tag{5}$$

where

$$\begin{aligned} K_1 &= \frac{(1+ge^{-j\theta})}{2}, \\ K_2 &= \frac{(1-ge^{j\theta})}{2}, \end{aligned} \tag{6}$$

and the symbol $*$ represents the complex conjugation. Note that the phase imbalance between I and Q falls in the range of $-\pi/4 \le \theta \le \pi/4$ [20]. The second term on the right-hand side of (5) is called the unwanted image of the signal, which causes performance degradation. Based on this model, some of the existing I/Q imbalance compensation algorithms estimate parameters K_1 and K_2 while others try to eliminate the second term by using adaptive filtering techniques [8, 12–16].

When both the frequency offset and the I/Q imbalance are involved, $s(n)$ and $s^*(n)$ in (5) should be replaced by $s(n)e^{j\varphi n}$ and $s^*(n)e^{-j\varphi n}$, respectively. As such, the received signal $y(n)$ can be modified as

$$y(n) = K_1 s(n)e^{j\varphi n} + K_2 s^*(n)e^{-j\varphi n} + w(n). \tag{7}$$

Due to the two exponential terms involved in (7), the received signal is no longer the rotated version of $s(t)$. In such a case, classical frequency estimators like the maximum likelihood estimator, cannot work properly. Moreover, unlike the signal model (5), the exponential terms in (7) make it difficult to estimate the I/Q imbalance using the methods in [15, 16].

In order to solve the estimation problem in (7), we now express the received signal as its inphase and quadrature components and attempt to explore the relationship between them for the development of a new estimation algorithm. Substituting (6) into (7), the inphase and quadrature components of $y(n)$ can be written as

$$y_i(n) = s_i(n)\cos\varphi n - s_q(n)\sin\varphi n + w_i(n), \tag{8}$$

$$y_q(n) = gs_i(n)\sin(\varphi n - \theta) + gs_q(n)\cos(\varphi n - \theta) + w_q(n), \tag{9}$$

where $w_i(n)$ and $w_q(n)$ are uncorrelated and zero-mean noises representing, respectively, the inphase and the quadrature components of $w(n)$. Clearly, when the system is free of frequency offset and the I/Q imbalance, (8) and (9) reduce to $y_i(n) = s_i(n) + w_i(n)$ and $y_q(n) = s_q(n) + w_q(n)$, respectively.

3. FREQUENCY OFFSET ESTIMATION

In a balanced I and Q quadrature receiver, the received signal only contains the frequency error $\Delta\omega$ and it can be regarded as a rotated version of transmitted signal. Thus, a classical estimation algorithm can be applied directly. However, when the I/Q imbalance exists, one has to consider both frequencies at $\omega - \Delta\omega$ and $\omega + \Delta\omega$. In this section, we present a carrier frequency offset estimator using the preamble defined in the IEEE802.11a standard. As specified in the standard, the preamble, consisting of 10 identical short symbols along with 2 long symbols, is transmitted before the information signal. The short symbols, each containing 16 data samples, are used to detect the start of a frame and carry out coarse frequency offset estimation, while the long symbols, each containing 64 samples, are employed for fine frequency correction, phase tracking, and channel estimation. Other 32 samples allocated between the short symbols and long symbols are used to eliminate intersymbol interference caused by short symbols. In this paper, only the short symbols are utilized.

3.1. Proposed algorithm

The channel is modelled as a linear time-invariant system within the preamble period, namely, the length of the channel impulse response is assumed to be smaller than one short symbol [4, 6]. Accordingly, the first received symbol should be discarded due to the channel induced intersymbol interference. Then, for the following $P-1$ short symbols ($P = 10$),

we have $s_i(n) = s_i(n + kM)$ and $s_q(n) = s_q(n + kM)$, where M represents the number of samples in each short symbol, n is limited within $[M + 1, 2M]$, and $k \in [0, P - 2]$. Therefore, the relationship among the short symbols can be given as

$$\begin{aligned} y_i(n + kM) &= s_i(n)\cos\varphi(n + kM) \\ &\quad - s_q(n)\sin\varphi(n + kM) + w_i(n + kM), \end{aligned} \tag{10}$$

$$\begin{aligned} y_q(n + kM) &= gs_i(n)\sin\left[\varphi(n + kM) - \theta\right] \\ &\quad + gs_q(n)\cos\left[\varphi(n + kM) - \theta\right] + w_q(n + kM). \end{aligned} \tag{11}$$

In what follows, we will derive a carrier frequency offset estimation algorithm based on (8)–(11).

Consider two sequences, $z_1(n)$ and $z_2(n)$, which are defined as

$$\begin{aligned} z_1(n) &= y_i(n + M)y_q(n) - y_i(n)y_q(n + M), \\ z_2(n) &= y_i(n + 2M)y_q(n) - y_i(n)y_q(n + 2M). \end{aligned} \tag{12}$$

Substituting (8)–(11) into (12), respectively, we obtain

$$z_1(n) = -g\left[s_i^2(n) + s_q^2(n)\right]\sin\varphi M\cos\theta + n_1(n) \tag{13}$$

with

$$\begin{aligned} n_1(n) &= \left[gs_i(n)\sin(\varphi n - \theta) + gs_q(n)\cos(\varphi n - \theta)\right]w_i(n + M) \\ &\quad + \left[s_i(n)\cos\varphi(n + M) - s_q(n)\sin\varphi(n + M)\right]w_q(n) \\ &\quad + w_i(n + M)w_q(n) \\ &\quad + \left[s_i(n)\cos\varphi n - s_q(n)\sin\varphi n\right]w_q(n + M) \\ &\quad + \{gs_i(n)\sin[\varphi(n + M) - \theta] \\ &\qquad + gs_q(n)\cos[\varphi(n + M) - \theta]\}w_i(n) \\ &\quad + w_i(n)w_q(n + M), \\ z_2(n) &= -g\left[s_i^2(n) + s_q^2(n)\right]\sin 2\varphi M\cos\theta + n_2(n) \end{aligned} \tag{14}$$

with

$$\begin{aligned} n_2(n) &= \left[gs_i(n)\sin(\varphi n - \theta) + gs_q(n)\cos(\varphi n - \theta)\right]w_i(n + 2M) \\ &\quad + \left[s_i(n)\cos\varphi(n + 2M) - s_q(n)\sin\varphi(n + 2M)\right]w_q(n) \\ &\quad + w_i(n + 2M)w_q(n) \\ &\quad + \left[s_i(n)\cos\varphi n - s_q(n)\sin\varphi n\right]w_q(n + 2M) \\ &\quad + \{gs_i(n)\sin[\varphi(n + 2M) - \theta] \\ &\qquad + gs_q(n)\cos[\varphi(n + 2M) - \theta]\}w_i(n) \\ &\quad + w_i(n)w_q(n + 2M). \end{aligned} \tag{15}$$

Taking the expectation of $z_1(n)$, one can obtain

$$E\{z_1(n)\} = -g\left[s_i^2(n) + s_q^2(n)\right]\sin\varphi M\cos\theta. \tag{16}$$

In obtaining (16), we have used the fact that $n_1(n)$ has a zero mean, since $w_i(n)$ and $w_q(n)$ are uncorrelated zero-mean noises and both are independent of $s_i(n)$ and $s_q(n)$. Similarly, we have

$$E\{z_2(n)\} = -g\left[s_i^2(n) + s_q^2(n)\right]\sin 2\varphi M\cos\theta. \tag{17}$$

Note that g is positive by definition and $\cos\theta$ is also a well-determined positive number due to the range of θ, that is, $[-\pi/4 \le \theta \le \pi/4]$. From (16) and (17), we obtain

$$\cos\varphi M = \frac{E\{z_2(n)\}}{2E\{z_1(n)\}}. \tag{18}$$

It is seen from (18) that the normalized frequency offset is well related to the means of $z_1(n)$ and $z_2(n)$. Accordingly, a reasonable estimate of the frequency offset can be given by

$$\hat{\varphi} = \Delta\omega T_s = \frac{1}{M}\cos^{-1}\frac{\sum_{n=M+1}^{M(P-2)} z_2(n)}{2\sum_{n=M+1}^{M(P-2)} z_1(n)}. \tag{19}$$

Note that there is a sign ambiguity in the frequency offset estimate using (19) due to the nonmonotonic mapping of $\cos^{-1}(x)$. However, the actual sign of the estimated frequency offset can easily be determined from the sign of $\sum_{n=M+1}^{M(P-2)} z_2(n)$. From (16) and (17), g, $\cos\theta$ and $[s_i^2(n)+s_q^2(n)]$ are all positive. Therefore, the sign of $\hat{\varphi}$ is opposite to the sign of $\sum_{n=M+1}^{M(P-2)} z_2(n)$. It should be mentioned that (19) is also applicable to the I/Q imbalance-free case, since the balanced case corresponding to $g = 1$ and $\theta = 0$ does not forfeit the use of $E[z_1(n)]$ and $E[z_2(n)]$ as seen from (16) and (17).

The frequency offset is usually measured by the ratio ε of the actual carrier frequency offset (Δf) to the subcarrier spacing $1/T_sN$, that is, $\varepsilon = T_sN\Delta f$, where T_s is the sampling period and N is the number of subcarriers. The estimate for ϕ given by (19) can then be translated into that for ε as shown below:

$$\hat{\varepsilon} = \frac{N}{2\pi M}\cos^{-1}\frac{\sum_{n=M+1}^{M(P-2)} z_2(n)}{2\sum_{n=M+1}^{M(P-2)} z_1(n)}. \tag{20}$$

It is seen from (19) and (20) that a total of $P-1$ short symbols has been used for the estimation as the result of dropping the first short symbol due to the channel-induced interference.

As will be seen from computer simulation in Section 5, the performance of the proposed CFO estimator for large CFOs is better than for small CFOs. This is because when the frequency error is large, both the numerator and denominator in the arccos function (20) are dominated by their first parts since the noise term is very small after sum operation. Therefore, the proposed estimator provides a more consistent CFO estimation. When the frequency error is small, both the numerator and the denominator are more dependent on the noise terms and therefore, the estimation result is less accurate. When ε is very close to zero (say ε <0.005), both numerator and denominator in (20) will approach to zero. The summations $\sum_{n=1}^{M(P-2)} z_2(n)$ and $2\sum_{n=1}^{M(P-2)} z_1(n)$ contain noise only and therefore the arccos function does not work properly. To ensure CFO estimator to give a meaningful

result when ε is near zero, a threshold Th is used to determine whether or not (20) should be employed. When $\sum_{n=1}^{M(P-2)} z_2(n)$ and $2\sum_{n=1}^{M(P-2)} z_1(n)$ are less than a threshold Th, the CFO estimator considers that the OFDM system has no frequency offset, that is, $\hat{\varepsilon} = 0$. Otherwise, the CFO estimate is given by (20). An appropriate threshold can be determined through simulations.

3.2. Analysis of the frequency offset estimator

3.2.1. Correction range and complexity

In order to avoid the phase ambiguity in the frequency offset estimation, the actual frequency error $2\varphi M$ should be within the range of $(-\pi, \pi)$ as seen from (17). Therefore, the correction range of $\varepsilon = N\varphi/2\pi$ is given by $(-N/4M, N/4M)$. From IEEE 802.11a standard, it is known that $M = 16$, $N = 64$, and the subcarrier spacing is 312.5 KHz. Thus, the correction range of ε is $(-1, 1)$, implying that the correctable frequency offset Δf varies from -312.5 to 312.5 KHz. In reality, considering the effect of noise, the actual correction range would be slightly smaller, say $-0.9 < \varepsilon < 0.9$. It is to be noted that most of the conventional frequency offset estimators have a correction capability of $|\varepsilon| < 0.5$ only.

In addition to correction range, computational complexity is another important factor evaluating an estimator. From (19), the number of multiplications required by the proposed estimator is approximately of the order of $4M(P-3)$. In contrast, the frequency offset estimator in [9] which also takes into account the I/Q imbalance seems computationally intensive. It requires at least several hundreds of searches to achieve an estimate given 1% estimation error, that is, $|\varepsilon - \hat{\varepsilon}| \le 0.01$. Moreover, the computational complexity for each search of the algorithm is of $O(M^3)$, where M is the number of data samples in each short symbol.

3.2.2. Mean

We now consider the mean value of $\cos M\hat{\varphi}$, namely,

$$E\{\cos\hat{\varphi}M\} = E\left\{\frac{\sum_{n=M+1}^{M(P-2)}\{g[s_i^2(n)+s_q^2(n)]\sin 2\varphi M\cos\theta + n_1(n)\}}{2\sum_{n=M+1}^{M(P-2)}\{g[s_i^2(n)+s_q^2(n)]\sin\varphi M\cos\theta + n_2(n)\}}\right\}$$

$$= E\left\{\frac{g\sin 2\varphi M\cos\theta\sum_{n=M+1}^{M(P-2)}[s_i^2(n)+s_q^2(n)] + \sum_{n=M+1}^{M(P-2)} n_1(n)}{2g\sin\varphi M\cos\theta\sum_{n=M+1}^{M(P-2)}[s_i^2(n)+s_q^2(n)] + \sum_{n=M+1}^{M(P-2)} n_2(n)}\right\}, \tag{21}$$

where $n_1(n)$ and $n_2(n)$ represent zero-mean additive noises. The sums $\sum_{n=M+1}^{M(P-2)} n_1(n)$ and $\sum_{n=M+1}^{M(P-2)} n_2(n)$ can be regarded as the time average of $n_1(n)$ and $n_2(n)$, and therefore, they approach zero when $M(P-3)$ is large enough. As a result, (21) can be simplified as

$$E\{\cos\hat{\varphi}M\} = E\left\{\frac{g\sin 2\varphi M\cos\theta(P-3)\sum_{n=1}^{M}[s_i^2(n)+s_q^2(n)]}{2g\sin\varphi M\cos\theta(P-3)\sum_{n=1}^{M}[s_i^2(n)+s_q^2(n)]}\right\}. \tag{22}$$

The summations in (22) represent the energy of one short symbol and can be regarded as constant. Thus, we have

$$E\{\cos\hat{\varphi}M\} = \frac{\sin 2\varphi M}{2\sin\varphi M} = \cos\varphi M. \tag{23}$$

Equation (23) indicates that the estimation of $\cos\varphi M$ is unbiased. As $\cos\varphi M$ and φ are one-to-one correspondence within the correction range, it can be concluded that the proposed estimator given by (19) and (20) is unbiased.

4. I/Q IMBALANCE COMPENSATION

In this section, a fast and efficient I/Q imbalance estimation algorithm is proposed by using the same short symbols as used for frequency offset estimation. Instead of estimating the amplitude mismatch g and the angular error θ directly, we will formulate the estimation problem for two unknowns $tg\theta$ and $1/g\cos\theta$. It will be shown that the I/Q imbalance can be more efficiently compensated in terms of the computational complexity by using the estimates of $tg\theta$ and $1/g\cos\theta$. The basic idea of estimating $tg\theta$ and $1/g\cos\theta$ is to establish a least-square problem by using the received symbols and the frequency offset estimate obtained in the previous section.

By expanding $\sin(\varphi n - \theta)$ and $\cos(\varphi n - \theta)$ in (9), the quadrature component of the received short symbols can be written as

$$\begin{aligned} y_q(n) = {} & g[s_i(n)\sin\varphi n + s_q(n)\cos\varphi n]\cos\theta \\ & - g[s_i(n)\cos\varphi n - s_q(n)\sin\varphi n]\sin\theta + w_q(n). \end{aligned} \tag{24}$$

Using (8), (24) can be rewritten as

$$\begin{aligned} y_q(n) = {} & g[s_i(n)\sin\varphi n + s_q(n)\cos\varphi n]\cos\theta \\ & - g y_i(n)\sin\theta + w_q(n) + g w_i(n)\sin\theta. \end{aligned} \tag{25}$$

Dividing both sides of (25) by $g\cos\theta$ and rearranging the terms lead to

$$y_i(n)U + y_q(n)V - w_1(n) = s_i(n)\sin\varphi n + s_q(n)\cos\varphi n, \tag{26}$$

where $U = tg\theta$, $V = 1/g\cos\theta$, and $w_1(n) = (w_q(n) + g\sin\theta w_i(n))/g\cos\theta$. As the knowledge about $s_i(n)$ and $s_q(n)$ involved in the right-hand side of (26) is not available to the receiver, they should be eliminated. In a manner similar to obtaining (26), using (10) and (11), we obtain

$$\begin{aligned} & y_i(n+M)U + y_q(n+M)V - w_1(n+M) \\ & \quad = s_i(n)\sin\varphi(n+M) + s_q(n)\cos\varphi(n+M). \end{aligned} \tag{27}$$

Expanding $\cos\phi(M+n)$ and $\sin\phi(M+n)$ in (27), and dividing both sides by $\cos\phi M$, we have

$$\begin{aligned} & \frac{y_i(n+M)}{\cos\varphi M}U + \frac{y_q(n+M)}{\cos\varphi M}V - \frac{w_i(n+M)}{\cos\varphi M} \\ & \quad = [s_i(n)\cos\varphi n - s_q(n)\sin\varphi n]tg\varphi M \\ & \qquad + [s_i(n)\sin\varphi n + s_q(n)\cos\varphi n]. \end{aligned} \tag{28}$$

By using (8) and (26) into the right-hand side of (28) and rearranging items, we obtain

$$\left[\frac{y_i(n+M)}{\cos\varphi M} - y_i(n)\right]U + \left[\frac{y_q(n+M)}{\cos\varphi M} - y_q(n)\right]V = y_i(n)tg\varphi M + w_2(n), \tag{29}$$

where $w_2(n) = w_1(n+M)/\cos\varphi M - w_1(n)$ represents the noise term. Clearly, $w_2(n)$ has a zero mean. Note that $\cos M\varphi$ and $\sin M\varphi$ can be replaced by their estimates $\cos M\hat{\varphi}$ and $\sin M\hat{\varphi}$. As a number of equations like (29) can be established with respect to different values of n, say, $n = M+1, M+2, \ldots, M(P-1)$, a least-square approximation problem for U and V can be readily formulated. According to (29), up to M linear equations can be established for each received short symbol, implying that a total of $M(P-2)$ linear equations is involved in the LS formulation if all the samples of short symbols are used. In order to reduce the impact of the noise on data samples and to decrease the number of equations in the LS problem, one can combine the M equations corresponding to the same symbol. Then, the number of equations is reduced to $P-2$. This procedure can be described as

$$a(l)U + b(l)V = c(l) + \psi(l) \quad l = 1, 2, \ldots, P-2, \tag{30}$$

where

$$\begin{aligned} a(l) &= \sum_{n=lM+1}^{lM+M}\left[y_i(n) - \frac{y_i(n+M)}{\cos M\varphi}\right] \\ b(l) &= \sum_{n=lM+1}^{lM+M}\left[\frac{y_q(n+M)}{\cos M\varphi} - y_q(n)\right] \\ c(l) &= \sum_{n=lM+1}^{lM+M} y_i(n)tgM\varphi \\ \psi(l) &= \sum_{n=lM+1}^{lM+M} w_2(n). \end{aligned} \tag{31}$$

Evidently, the linear system (30) can be rewritten in the matrix form as

$$\mathbf{H}\begin{bmatrix} U \\ V \end{bmatrix} + \boldsymbol{\Psi} = \mathbf{c}, \tag{32}$$

where $\mathbf{H}[\mathbf{a}, \mathbf{b}]$ with $\mathbf{a} = [a(1), \ldots, a(P-1)]^T$ and $\mathbf{b} = [b(1), \ldots, b(P-1)]^T$, and $\mathbf{c} = [c(1), \ldots, c(P-1)]^T$. In (32), $\mathbf{H}$ and $\mathbf{c}$ are known, $\boldsymbol{\Psi}$ is a zero-mean noise vector, and $[\cdot]^T$ denotes the matrix transpose. Solving (32) leads to a least-square solution for U and V, that is,

$$\begin{bmatrix} U \\ V \end{bmatrix} = (\mathbf{H}^T\mathbf{H})^{-1}\mathbf{H}^T\mathbf{c}. \tag{33}$$

We now show that once the parameters U and V are estimated, the I/Q imbalance in the received signal can be easily eliminated. Denoting the transmitted and the received information signals as $s^i(n)$ and $y^i(n)$, respectively, the I and Q components of the received signal can be written as

$$\begin{aligned} \begin{bmatrix} y_i^i(n) \\ y_q^i(n) \end{bmatrix} &= \begin{bmatrix} s_i^i(n)\cos\varphi n - s_q^i(n)\sin\varphi n \\ gs_i^i(n)\sin(\varphi n - \theta) + gs_q^i(n)\cos(\varphi n - \theta) \end{bmatrix} + \begin{bmatrix} w_i(n) \\ w_q(n) \end{bmatrix} \\ &= \begin{bmatrix} 0 & 1 \\ g\cos\theta & -g\sin\theta \end{bmatrix}\begin{bmatrix} \sin\varphi n & \cos\varphi n \\ \cos\varphi n & -\sin\varphi n \end{bmatrix}\begin{bmatrix} s_i^i(n) \\ s_q^i(n) \end{bmatrix} + \begin{bmatrix} w_i(n) \\ w_q(n) \end{bmatrix}, \end{aligned} \tag{34}$$

where y_i^i and y_q^i are the inphase and quadrature components of received information signal, and s_i^i and s_q^i the inphase and quadrature components of the transmitted information signal. Note that the frequency offset of the received signal can be corrected in the frequency estimation stage by using an existing CFO compensation algorithm such as that suggested in [19]. Then, the received information signal can be written as

$$\begin{bmatrix} y_i^i(n) \\ y_q^i(n) \end{bmatrix} = \begin{bmatrix} 0 & 1 \\ g\cos\theta & -g\sin\theta \end{bmatrix}\begin{bmatrix} 0 & 1 \\ 1 & 0 \end{bmatrix}\begin{bmatrix} s_i^i(n) \\ s_q^i(n) \end{bmatrix} + \begin{bmatrix} w_i(n) \\ w_q(n) \end{bmatrix}. \tag{35}$$

From (35), one can obtain the desired information signal as given by

$$\begin{bmatrix} s_i^i(n) \\ s_q^i(n) \end{bmatrix} = \begin{bmatrix} 1 & 0 \\ U & V \end{bmatrix}\begin{bmatrix} y_i^i(n) \\ y_q^i(n) \end{bmatrix} + \begin{bmatrix} w_i'(n) \\ w_q'(n) \end{bmatrix}, \tag{36}$$

where $w_i'(n)$ and $w_q'(n)$ denote the uncorrelated additive noises with zero mean. Clearly, (36) gives the recovered information signal if the noise terms are neglected.

5. SIMULATION RESULTS

In this section, computer simulations are carried out to validate the proposed algorithms. According to the IEEE 802.11a standard, the preamble contains $P = 10$ short symbols, each consisting of $M = 16$ data samples. Each OFDM symbol contains 80 samples out of which 64 are for the 64 subchannels and 16 for cyclic prefix. The sampling frequency is $1/T_s = 20$ MHz. The carrier frequency offset is normally measured by the ratio ε of the actual frequency offset to the subcarrier spacing. For the purpose of comparison with existing methods, the absolute value of ε is limited to 0.5 in our simulation although the proposed frequency offset estimation algorithm allows for a maximum value of $\varepsilon = 1$. The multipath channel is modeled as a three-ray FIR filter.

Experiment 1 (performance of the frequency offset estimator). In this experiment, we would like to evaluate the average and mean-square error (MSE) of the proposed frequency offset estimate as well as its robustness against the I/Q imbalance. The I/Q imbalance assumed here consists of 1 dB

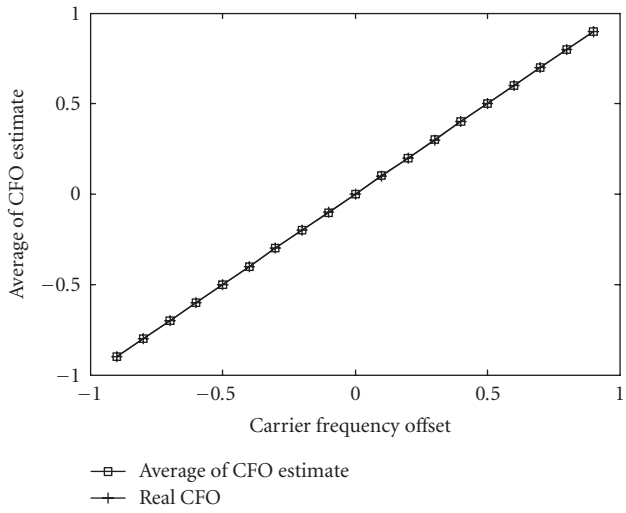

Figure 2: Average of CFO estimate (SNR = 20 dB, $g = 1$ dB, and $\theta = 15^\circ$).

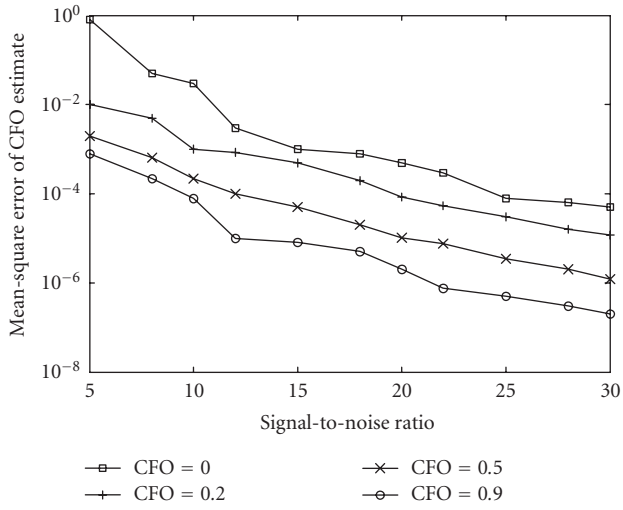

Figure 3: MSE of CFO estimate ($g = 1$ dB and $\theta = 15^\circ$).

amplitude error and 15° phase error. Figure 2 shows the average of frequency estimates resulting from 500 runs, where the signal-to-noise ratio (SNR) is set to 20 dB. As seen from Figure 2, it is confirmed that the proposed method is unbiased. Figure 3 depicts the MSE of the frequency offset estimate as a function of SNR. As expected, the MSE decreases significantly as the SNR increases.

Figure 4 shows the simulation results of the proposed method along with those from algorithms in [6, 7, 9, 17] for comparison, where the I/Q imbalance is assumed as $g = 0.1$ dB and $\theta = 5^\circ$, which represents a typical case of light I/Q imbalance. Similarly, Figure 5 gives the comparison result for the case of a heavy I/Q imbalance, namely, $g = 1$ dB and $\theta = 15^\circ$. The SNR is set to 20 dB in Figures 4 and 5. It is seen from Figures 4 and 5 that the performance of the

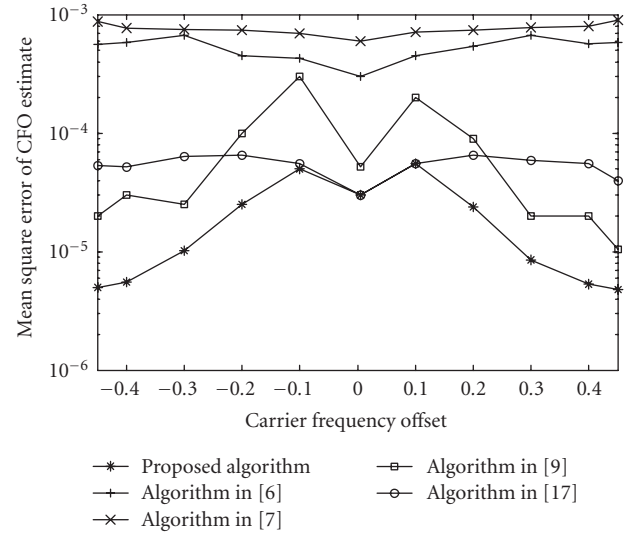

Figure 4: MSE comparison of CFO estimation algorithms with light I/Q imbalance ($g = 0.1$ dB and $\theta = 5^\circ$).

proposed method is affected by the actual frequency offset. When the frequency offset is relatively large, the MSE of the proposed estimate is smaller than that of the algorithms reported in [9, 17]. When the frequency offset is very small, the proposed method yields a performance that is similar to that of the existing algorithms. It is seen from above two figures that the CFO estimation algorithms proposed in [6, 7] result in a poor estimation performance. This is because the two estimators have used, respectively, nonlinear square algorithm and the maximum likelihood algorithm, both without considering the I/Q imbalance.

In order to measure the robustness of the proposed method against the I/Q imbalance, a set of values for g and θ is considered. It is assumed that $\varepsilon = 0.2$. Table 1 lists the MSE of the frequency offset estimate with the amplitude error of the I/Q imbalance varying from −3 dB to +3 dB and the phase error from −45° to 45°. It is observed that the estimated frequency offset almost does not depend on the I/Q imbalance. The minimum and the maximum MSEs of the frequency estimate are 0.1937×10^{-4} and 0.2877×10^{-4}, respectively, which indicates a very small estimation deviation considering a significant range of both the amplitude and the phase errors as shown in the table. Therefore, the proposed algorithm has a very good robustness to the I/Q imbalance.

Experiment 2 (performance of the I/Q imbalance estimation). In this experiment, simulation results in terms of the average and MSE of the estimates of two parameters U and V are provided to show the performance of the proposed method. Also, the computational complexity of the I/Q imbalance estimation is discussed. The I/Q imbalance is assumed as $g = 1$ dB and $\theta = 15^\circ$. Figure 6 shows the MSE of U, V, and the frequency offset where the SNR varies from 10 dB to 25 dB. As seen in Figure 6, the MSE of the estimates decreases as SNR increases, and the MSE of U and V

Table 1: MSE ($\times 10^{-4}$) of CFO estimate with various I/Q imbalances ($\varepsilon = 0.2$ and SNR = 20 dB). (Minimum and maximum values are highlighted.)

	Amplitude (dB)						
Phase (°C)	−3	−2	−1	0	1	2	3
−45	0.2458	0.2382	0.2502	0.2609	0.2304	0.2347	0.1859
−35	0.2284	0.2486	0.2127	0.2165	0.2141	0.2323	0.2387
−25	0.2629	0.2111	0.2732	0.2688	0.2308	0.2364	0.2718
−15	0.2028	0.2511	0.2229	0.2252	0.2382	0.2767	0.251
−5	0.2095	0.2221	0.251	0.2093	0.2398	0.2279	0.2638
0	0.2452	0.2288	0.1941	0.2621	**0.2877**	0.2314	0.2419
5	0.2418	0.2028	0.2378	0.2521	0.2392	0.2644	0.2314
15	0.2286	0.2009	0.2492	0.2521	0.2392	0.2644	0.249
25	0.2586	0.2217	0.2526	0.2722	0.2709	0.2635	0.24
35	**0.1937**	0.2169	0.2558	0.2558	0.2427	0.2706	0.2566
45	0.2072	0.2365	0.2335	0.2773	0.2536	0.2357	0.2254

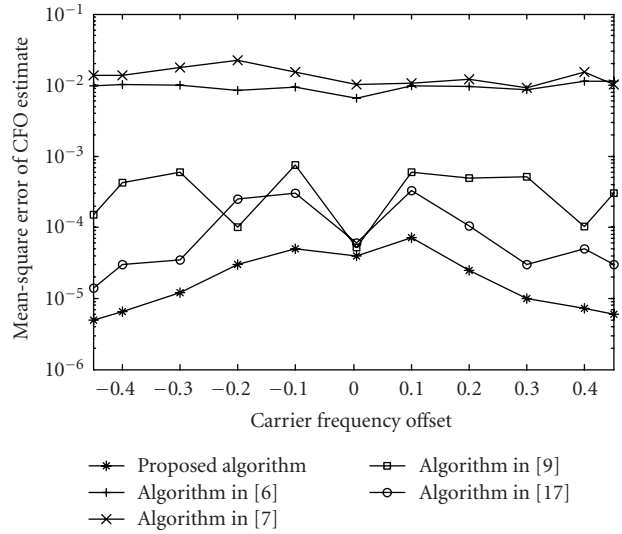

Figure 5: MSE comparison of CFO estimation algorithms with heavy I/Q imbalance ($g = 1$ dB and $\theta = 15°$).

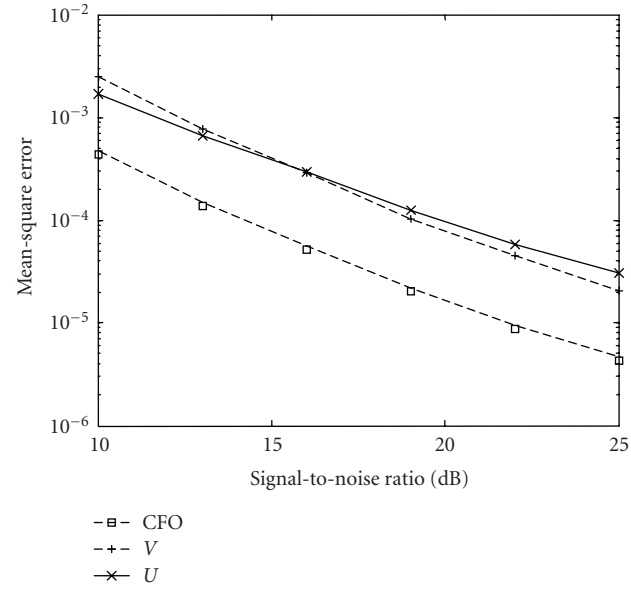

Figure 6: MSE of I/Q imbalance estimate versus SNR ($U = tg\theta$, $V = 1/g\cos\theta$, and $\varepsilon = 0.3$).

estimates are larger than that of the frequency estimate, since the estimated frequency offset has been used in the I/Q imbalance estimation stage.

Figures 7 and 8 show, respectively, the average and the MSE plots of the estimates of U and V as a function of the number of short symbols used for the I/Q imbalance estimation, where ε is set to 0.3 and SNR 20 dB. As shown in Figure 7, the estimates of U and V are unbiased. Furthermore, their averages are not affected by the number of short symbols used. On the other hand, as shown in Figure 8, the MSE values are very large if a small number of short symbols is used. When the number is increased to 5, the MSE performance can be improved considerably. However, if the number is further increased, the MSE performance only changes slightly. Therefore, a large number of short symbols is not recommended in view of the computational complexity of the I/Q imbalance estimation. It appears that $5 \sim 7$ short symbols are a good tradeoff between the estimation performance and the computational load.

Experiment 3 (BER performance of OFDM systems using the proposed algorithms). In this experiment, we would like to show the bit-error rate (BER) of an OFDM system using the proposed frequency offset and I/Q imbalance estimation/compensation algorithms. Each OFDM frame is assumed to contain 10 short symbols followed by 10 OFDM symbols. The I/Q imbalance is assumed as $g = 1$ dB and $\theta = 15°$. Figure 9 shows the BER-SNR plots of a BPSK OFDM system with and without the proposed I/Q imbalance

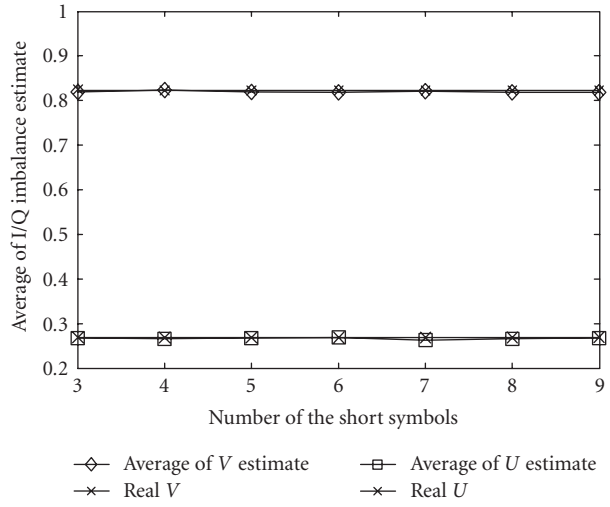

Figure 7: Average of I/Q imbalance estimate verses number of short symbols used ($U = tg\theta$, $V = 1/g\cos\theta$, and $\varepsilon = 0.1$).

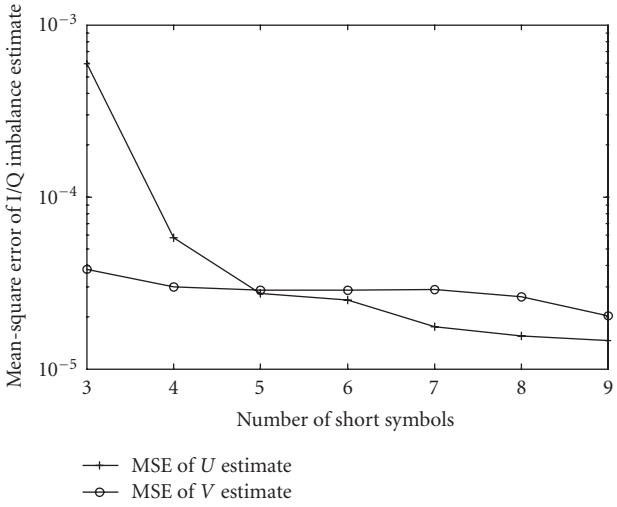

Figure 8: MSE of I/Q imbalance estimate versus number of short symbols used ($U = tg\theta$ and $V = 1/g\cos\theta$).

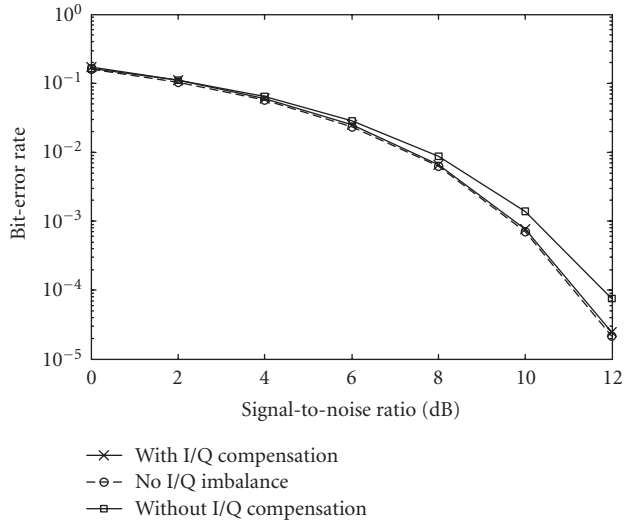

Figure 9: BER performance of a BPSK OFDM system with I/Q imbalance correction.

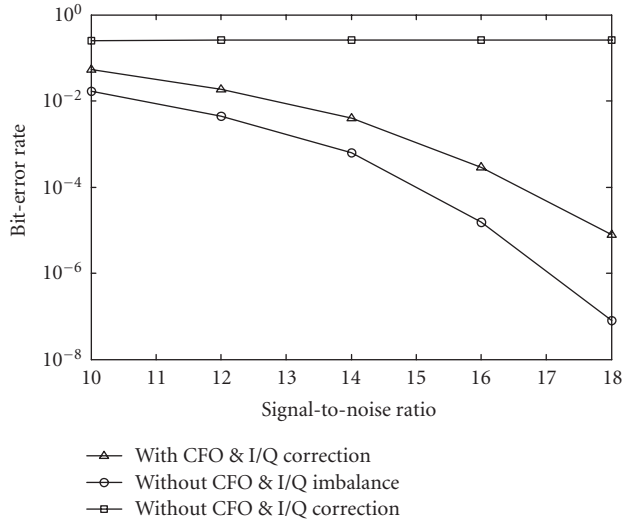

Figure 10: BER performance of a 16 QAM OFDM system with CFO and I/Q imbalance correction.

correction. It is clear that the BER performance of the OFDM system with I/Q imbalance compensation is very close to the ideal case which has no I/Q imbalance.

Figure 10 shows the overall BER performances of a 16-QAM OFDM system when both frequency offset and I/Q imbalance are involved. The frequency offset ε is set to 0.2, the amplitude imbalance is 0.5 dB, and the phase imbalance is 15°. The scheme proposed in [19] has been employed to correct the carrier frequency offset. It is seen from Figure 10 that, by using the proposed scheme, the degradation of the BER performance of the entire system is only about 2 dB when the SNR is less than 14 dB, and it is less than 2 dB as the SNR gets larger.

6. CONCLUSION

In this paper, we have presented a low-cost and preamble-aided algorithm for the estimation/compensation of carrier frequency offset and I/Q imbalance in OFDM systems. It has been shown that the proposed frequency offset estimator is fast, efficient, and robust to I/Q imbalance, thus reducing the design pressure for local mixer. By using the same preamble along with a least-square algorithm, the I/Q imbalance has also been estimated quickly and efficiently. The distinct feature of the proposed method is its computational efficiency and fast implementation and is, therefore, particularly suitable for realization in burst-mode transmission systems. It

should be mentioned that the proposed technique can easily be extended for applications in other communication systems as long as those systems have a similar preamble structure.

ACKNOWLEDGMENT

This work was supported by the Natural Sciences and Engineering Research Council (NSERC) of Canada.

REFERENCES

[1] J. Heiskala and J. Terry, *OFDM Wireless LANs: A Theoretical and Practical Guide*, SAMS, Indianapolis, Indiana, 2002.

[2] J.-J. Van De Beek, M. Sandell, and P. O. Börjesson, "ML estimation of time and frequency offset in OFDM systems," *IEEE Transactions on Signal Processing*, vol. 45, no. 7, pp. 1800–1805, 1997.

[3] H. Minn, V. K. Bhargava, and K. B. Letaief, "A robust timing and frequency synchronization for OFDM systems," *IEEE Transactions on Wireless Communications*, vol. 2, no. 4, pp. 822–839, 2003.

[4] N. Lashkarian and S. Kiaei, "Class of cyclic-based estimators for frequency-offset estimation of OFDM systems," *IEEE Transactions on Communications*, vol. 48, no. 12, pp. 2139–2149, 2000.

[5] X. Ma, C. Tepedelenlioğlu, G. B. Giannakis, and S. Barbarossa, "Non-data-aided carrier offset estimators for OFDM with null subcarriers: identifiability, algorithms, and performance," *IEEE Journal on Selected Areas in Communications*, vol. 19, no. 12, pp. 2504–2515, 2001.

[6] J. Li, G. Liu, and G. B. Giannakis, "Carrier frequency offset estimation for OFDM-based WLANs," *IEEE Signal Processing Letters*, vol. 8, no. 3, pp. 80–82, 2001.

[7] A. J. Coulson, "Maximum likelihood synchronization for OFDM using a pilot symbol: algorithms," *IEEE Journal on Selected Areas in Communications*, vol. 19, no. 12, pp. 2486–2494, 2001.

[8] M. Valkama, M. Renfors, and V. Koivunen, "Advanced methods for I/Q imbalance compensation in communication receivers," *IEEE Transactions on Signal Processing*, vol. 49, no. 10, pp. 2335–2344, 2001.

[9] G. Xing, M. Shen, and H. Liu, "Frequency offset and I/Q imbalance compensation for OFDM direct-conversion receivers," in *Proceedings of IEEE International Conference on Acoustics, Speech and Signal Processing (ICASSP '03)*, vol. 4, pp. 708–711, Hong Kong, April 2003.

[10] C.-L. Liu, "Impacts of I/Q imbalance on QPSK-OFDM-QAM detection," *IEEE Transactions on Consumer Electronics*, vol. 44, no. 3, pp. 984–989, 1998.

[11] V. K.-P. Ma and T. Ylamurto, "Analysis of IQ imbalance on initial frequency offset estimation in direct down-conversion receivers," in *Proceedings of the 3rd IEEE Workshop on Signal Processing Advances in Wireless Communications (SPAWC '01)*, pp. 158–161, Taiwan, China, March 2001.

[12] M. Valkama, M. Renfors, and V. Koivumen, "Compensation of frequency-selective I/Q imbalances in wideband receivers: models and algorithms," in *Proceedings of the 3rd IEEE Workshop on Signal Processing Advances in Wireless Communications (SPAWC '01)*, pp. 42–45, Taiwan, China, March 2001.

[13] A. R. Wright and P. A. Naylor, "I/Q mismatch compensation in zero-IF OFDM receivers with application to DAB," in *Proceedings of IEEE International Conference on Acoustics, Speech and Signal Processing (ICASSP '03)*, vol. 2, pp. 329–332, Hong Kong, April 2003.

[14] J. Tubbax, B. Come, L. Van der Perre, L. Deneire, S. Donnay, and M. Engels, "Compensation of IQ imbalance in OFDM systems," in *Proceedings of International Conference on Communications (ICC '03)*, vol. 5, pp. 3403–3407, Anchorage, Alaska, USA, May 2003.

[15] H. Shaflee and S. Fouladifard, "Calibration of IQ imbalance in OFDM transceivers," in *Proceedings of IEEE International Conference on Communications (ICC '03)*, vol. 3, pp. 2081–2085, Seattle, Wash, USA, May 2003.

[16] C. C. Gaudes, M. Valkama, and M. Renfors, "A novel frequency synthesizer concept for wireless communications," in *Proceedings of IEEE International Symposium on Circuits and Systems (ISCAS '03)*, vol. 2, pp. 85–88, Bangkok, Thailand, May 2003.

[17] J. Tubbax, A. Fort, L. Van der Perre, et al., "Joint compensation of IQ imbalance and frequency offset in OFDM systems," in *Proceedings of IEEE Global Telecommunications Conference (GLOBECOM '03)*, vol. 4, pp. 2365–2369, San Francisco, Calif, USA, December 2003.

[18] S. Fouladifard and H. Shafiee, "Frequency offset estimation in OFDM systems in presence of IQ imbalance," in *Proceedings of the 8th International Conference on Communication Systems (ICCS '02)*, vol. 1, pp. 214–218, Amsterdam, The Netherlands, November 2002.

[19] J. Tubbax, L. Van der Perre, S. Donnay, M. Engels, M. Moonen, and H. De Man, "Joint compensation of IQ imbalance, frequency offset and phase noise in OFDM receivers," *European Transactions on Telecommunications*, vol. 15, no. 3, pp. 283–292, 2004.

[20] A. A. Abidi, "Direct-conversion radio transceivers for digital communications," *IEEE Journal of Solid-State Circuits*, vol. 30, no. 12, pp. 1399–1410, 1995.

Feng Yan received the B. Eng. degree from Northeast Electrical Power Institute, Jilin, China in 1991 and M. Eng. degree from Concordia University, Montreal, Canada in 2001, both in electrical engineering. He is currently working in the area of signal processing for wireless communication toward his Ph.D. degree. His research interests include synchronization techniques in OFDM communication systems and wireless networking.

Wei-Ping Zhu received the B.E. and M.E. degrees from Nanjing University of Posts and Telecommunications, and the Ph.D. degree from Southeast University, Nanjing, China in 1982, 1985 and 1991, respectively, all in electrical engineering. He was a Postdoctoral Fellow from 1991 to 1992 and a Research Associate from 1996 to 1998 in the Department of Electrical and Computer Engineering, Concordia University, Montreal, Canada. During 1993–1996, he was an Associate Professor in the Department of Information Engineering, Nanjing University of Posts and Telecommunications. From 1998 to 2001, he worked in hi-tech companies in Ottawa, Canada, including Nortel Networks and SR Telecom Inc. Since July 2001, he has been with Concordia's Electrical and Computer Engineering Department as an Associate

Professor. His research interests include signal processing algorithms and applications in wireless communication. He is a Senior Member of IEEE.

M. Omair Ahmad received the B.Eng. degree from Sir George Williams University, Montreal, P.Q., Canada, and the Ph.D. degree from Concordia University, Montreal, P.Q., Canada, both in electrical engineering. During 1978-1979, he was a Member of the Faculty of the New York University College, Buffalo. In September 1979, he joined the Faculty of Concordia University, where he was an Assistant Professor of Computer Science. Subsequently, he joined the Department of Electrical and Computer Engineering of the same university, where he was the Chair of the department from June 2002 to May 2005 and presently he is a Professor. He has published extensively in the area of signal processing and holds four patents. His current research interests include the areas of multidimensional filter design, speech, image and video processing, nonlinear signal processing, communication DSP, artificial neural networks, and VLSI circuits for signal processing. He was Founding Researcher in Micronet from its inception in 1999 as a Canadian Network of Centers of Excellence until its expiration in 2004. He was an Associate Editor of IEEE Transactions on Circuits and Systems Part I: Fundamental Theory and Applications from June 1999 to December 2001. Dr. Ahmed is a Fellow of IEEE.